Preparation and Evaluation of ^{68}Ga-DOTA-hEGF for Visualization of EGFR Expression in Malignant Tumors

Irina Velikyan, PhD[1,2]; Åsa Liljegren Sundberg, PhD[3]; Örjan Lindhe, PhD[2]; A. Urban Höglund, PhD[2]; Olof Eriksson, MS[2]; Eva Werner, MS[2]; Jorgen Carlsson, PhD[3]; Mats Bergström, PhD[2]; Bengt Långström, PhD[1,2]; and Vladimir Tolmachev, PhD[3]

[1]Department of Organic Chemistry, Institute of Chemistry, Biomedical Centre, Uppsala University, Uppsala, Sweden; [2]Uppsala Imanet AB, Uppsala, Sweden; and [3]Division of Biomedical Radiation Sciences, Uppsala University, Uppsala, Sweden

Detection of epidermal growth factor receptor (EGFR) overexpression in many carcinomas provides important diagnostic information, which can influence patient management. The use of PET may enable such detection in vivo by a noninvasive procedure with high sensitivity. The aim of this study was to develop a method for preparation of a positron-emitting tracer based on a natural ligand to EGFR, the recombinant human epidermal growth factor (hEGF), and to perform a preclinical evaluation of the tracer. **Methods:** DOTA-hEGF (DOTA is 1,4,7,10-tetraazacyclododecane-*N*,*N*′,*N*″,*N*‴-tetraacetic acid) was prepared by coupling of a *N*-sulfosuccinimide ester of DOTA to hEGF. The conjugate was labeled with a generator-produced positron-emitting nuclide, ^{68}Ga (half-life = 68 min), using microwave heating. Binding specificity, affinity, internalization, and retention of ^{68}Ga-DOTA-hEGF was studied in 2 EGFR-expressing cell lines, U343 glioma cells and A431 cervical carcinoma cells. Biodistribution and microPET visualization studies were performed in BALB/c *nu*/*nu* mice bearing A431 carcinoma xenografts. **Results:** A 1-min-long microwave-assisted labeling provided radioactivity incorporation of 77% ± 4%. Both cell lines demonstrated receptor-specific uptake of the conjugate, rapid internalization of the tracer, and good retention of radioactivity. Binding to both cell lines occurred with high affinity, approximately 2 nmol/L. The biodistribution study demonstrated accumulation of radioactivity in xenografts and in EGFR-expressing organs. The microPET imaging study enabled visualization of tumors and demonstrated quick—within 5 min—localization of radioactivity in tumors. **Conclusion:** ^{68}Ga-DOTA-hEGF has potential for imaging EGFR overexpression in tumors.

Key Words: ^{68}Ga; epidermal growth factor; PET; microPET; malignant tumors

J Nucl Med 2005; 46:1881–1888

The epidermal growth factor receptor (EGFR, HER1, ErbB-1) is a transmembrane protein of the tyrosine kinase receptor family. Activation of EGFR causes signaling that may lead to cell division, increasing motility and suppression of apoptosis (*1*). In several carcinomas, amplification or translocation of EGFR genes causes an increased transcription and a subsequent high level of EGFR expression (*2,3*). Such overexpression is documented in, for example, carcinomas of breast and lung (*4–6*). A high level of EGFR expression provides malignant cells with an advantage in survival by increasing cell proliferation and metastatic spread and decreased apoptosis. For the moment, several approaches to suppress tumor growth by inactivation of EGFR signaling are in clinical use or under evaluation. These approaches are based on either blocking ligand binding to the EGFR extracellular domain using anti-EGFR antibodies or preventing intracellular signaling with selective tyrosine kinase inhibitors (*7*).

EGFR expression in tumors has documented prognostic and predictive value. It has been shown that such overexpression is associated with poor survival and recurrences in non–small cell lung cancer (NSCLC) and breast cancer (*5,8,9*). Apparently, detection of EGFR in clinical practice might influence patient management, including questions of the relevance of the use of EGFR-targeted drugs.

Detection of EGFR is possible in surgical samples or samples of fine-needle biopsies using immunohistochemical or fluorescent in situ hybridization techniques. However, we believe that nuclear medicine visualization may provide advantages because of evaluation of the whole volume of both the primary tumor and the metastases, avoiding false-negative results associated with sampling errors and heterogeneity of EGFR expression.

The ^{111}In-labeled anti-EGFR antibody 425 was successfully used for detection of malignant gliomas (*10*). ^{99m}Tc-Labeled anti-EGFR humanized antibodies hR3 and C225 are under clinical evaluation (*11,12*). It should be noted, however, that the use of a bulky antibody might complicate radioconjugate diffusion through healthy tissues and into tumors. An alternative to anti-EGFR antibodies might be the use of a natural ligand, human epidermal growth factor (hEGF), as a targeting vector for delivery of radionuclides to tumor cells (*13*). The molecular weight of hEGF, 6.2

Received Mar. 14, 2005; revision accepted Jul. 15, 2005.
For correspondence or reprints contact: Bengt Långström, PhD, Uppsala Imanet, P.O. Box 967, SE-751 09 Uppsala, Sweden.
E-mail: Bengt.Langstrom@uppsala.imanet.se

kDa, might enable fast tumor penetration and fast blood clearance, providing good contrast of the image. Earlier, ^{131}I-labeled hEGF has been used successfully for visualization of lung cancer (*14*). However, poor cellular retention of radiohalogens might lead to decreased tumor accumulation and suboptimal imaging contrast, and the use of radiometals might be a better choice for labeling of hEGF (*15*). Thus, single-photon radiometal labels such as ^{111}In (half-life [$t_{1/2}$] = 2.8 d) and ^{99m}Tc ($t_{1/2}$ = 6 h) have previously been attached to hEGF (*15–20*). It might be advantageous, however, to use a positron-emitting label for hEGF, as PET is a superior detection technique in sensitivity, resolution, and quantification compared with SPECT (*21,22*).

An attractive positron-emitting label for hEGF might be ^{68}Ga ($t_{1/2}$ = 68 min). The half-life of this nuclide is compatible with the quick blood clearance of hEGF. ^{68}Ga possesses high positron emission (89%) and is readily available from a commercial ^{68}Ge/^{68}Ga generator (^{68}Ge, $t_{1/2}$ = 270.8 d) (*23,24*). The use of derivatives of macrocyclic chelators provided stable gallium labeling of somatostatin analogs and oligonucleotides (*24–26*).

Because of the short half-life of ^{68}Ga, the labeling time is important. To accelerate the chelating, microwave heating was used. This technique was shown previously to be efficient for 1,4,7,10-tetraazacyclododecane-*N,N′,N″,N‴*-tetraacetic acid (DOTA)-mediated ^{68}Ga labeling of oligonucleotides and peptides (*24,26,27*).

This study was performed with the intention of creating a positron-emitting ^{68}Ga-labeled conjugate of hEGF and evaluating the feasibility for the visualization of EGFR- expressing tumors.

MATERIALS AND METHODS

Materials

hEGF was purchased from Chemicon. Sodium acetate (99.995%), 4-(2-hydroxyethyl)piperazine-1-ethanesulfonic acid (HEPES), and double-distilled hydrochloric acid (Riedel de Haën) were obtained from Sigma-Aldrich Sweden. Sodium dihydrogen phosphate, disodium hydrogen phosphate, and trifluoroacetic acid (TFA) were obtained from Merck. The *N*-hydroxysuccinimide ester of DOTA (1,4,7,10-tetraazacyclododecane-1,4,7,10-tetraacetic acid) was purchased from Macrocyclics. The purchased chemicals were used without further purification. Deionized water (18.2 MΩ), produced with a Purelab Maxima Elga system was used in all reactions. ^{68}Ga was obtained from a commercial ^{68}Ge/^{68}Ga generator with 1.85 GBq ^{68}Ge-loaded activity and a 2- to 3-y shelf-life (Cyclotron C; Obninsk).

Preparation of ^{68}Ga-DOTA-hEGF

hEGF (32–70 nmol, 80–180 μL) in 0.08 mol/L borate buffer, pH 9.4, was added to dry *N*-hydroxysulfosuccinimide ester of DOTA (10- to 20-fold excess) under stirring, and the pH was further adjusted to 9.0 by adding borate buffer (240–340 μL). The mixture was left at room temperature for 3–4 h or overnight. The conjugate was purified on a Bio-Select RP C18 SPE column (Vydac). The reaction mixtures were passed slowly though the extraction disk, which was then washed with 2 mL of 0.1% TFA. The product was eluted in 1 mL of 70% acetonitrile with 0.1% TFA. The solvent was evaporated using a vacuum centrifuge (Labconco CentriVap Console), operated at 50°C, and the dry purified product was stored at a temperature below zero. Alternatively, the conjugate was purified and concentrated by ultracentrifugation through a filter with a molecular weight cutoff of 3,000 Da (Centricon-3; Amicon) against 3 changes of 12 mmol/L HEPES buffer. The filtration fractions were analyzed by reversed-phase high-performance liquid chromatography (RP-HPLC).

The labeling of the conjugate was performed using either nonconcentrated ^{68}Ga-eluate or eluate preconcentrated, as described previously (*24*). In some cases, the eluates from 2 generators were preconcentrated to increase the amount of ^{68}Ga used in the labeling reaction. The amount of DOTA-hEGF used in the labeling reaction was 6–10 and 2–5 nmol, respectively, when using nonconcentrated and preconcentrated ^{68}Ga-eluate, respectively. Sodium acetate buffer, pH 5.0–5.5, was used for labeling with nonconcentrated ^{68}Ga, and HEPES buffer, pH 4.6–4.8, was used for preconcentrated eluate. The labeling was performed at 90°C ± 5°C under microwave heating for 1 min. The product was purified on a Bio-Select RP C18 SPE column as described. The solvent was then changed to phosphate-buffered saline (PBS) on NAP-5 columns (Sephadex G-25; Amersham Pharmacia Biotech AB). The radiochemical purity of ^{68}Ga-DOTA-hEGF was assessed by UV-radio-HPLC, and the concentration of the conjugate and the tracer was determined from UV-HPLC standard plots.

To verify that the binding of ^{68}Ga to hEGF was DOTA mediated, a blank experiment was performed. The procedures were the same as described, but nonconjugated hEGF was used.

^{69,71}Ga of natural isotope composition was complexed to DOTA-hEGF using the same protocol. ^{69,71}Ga-DOTA-hEGF, characterized with liquid chromatography electrospray ionization mass spectrometry (LC-ESI-MS), was used for the identification of the radio-HPLC chromatogram signals.

HPLC Analysis

Analytic LC was performed using an HPLC system from Beckman consisting of a 126 pump, a 166 UV detector, and a radiation detector coupled in series. Data acquisition and handling were performed using the Beckman System Gold Nouveau Chromatography Software Package. The column used was a Vydac RP 300-Å HPLC column (Vydac) with the dimensions 150 × 4.6 mm, 5-μm particle size. The applied gradient elution had the following parameters: A = 10 mmol/L TFA; B = 70% acetonitrile (MeCN), 30% H_2O, 10 mmol/L TFA with UV detection at 220 nm; the flow rate was 1.2 mL/min; 0–2 min isocratic 20% B, 20%–90% B linear gradient 8 min, 90%–20% B linear gradient 2 min. The quantity of ^{68}Ga-DOTA-hEGF and radioimpurities retained on the column were controlled.

Microwave Heating

Microwave heating was performed in a SmithCreator monomodal microwave cavity producing continuous irradiation at 2,450 MHz (Biotage AB).

LC-ESI-MS Analysis

LC-ESI-MS was performed using the Waters Micromass Quattro Premier Mass Spectrometer (Micromass) and an HPLC system from Alliance (Waters 269) with a Photodiode Array UV detector. The column used was an Atlantis, dC 18, RP-HPLC column with the dimensions 100 × 2.1 mm, 3-μm particle size. Isocratic elution was applied with the following parameters: A = 10 mmol/L formic acid; B = 100% MeCN, with UV detection at 210–400

nm; the flow rate was 0.3 mL/min. LC-ESI-MS was performed with positive-mode scanning and selected ion recording detecting $[M+6H]^{6+}$, $[M+7H]^{7+}$, and $[M+8H]^{8+}$ ions of hEGF, $(DOTA)_n$-hEGF, and $(Ga\text{-}DOTA)_n$-hEGF, where $n = 1;2;3$. Reconstitution of the data gave molecular weight of 6,244.67 ± 1.15; 6,629.95 ± 0.05; 7,016 ± 0.08; 7,402 ± 0.1; 6,699.95 ± 0.05; 7,157.55 ± 2.47; 7,612.31 ± 0.05, respectively, for hEGF, $(DOTA)_n$-hEGF and $(Ga\text{-}DOTA)_n$-hEGF.

Cell Cultures

The human squamous carcinoma cell line A431 (CLR 1555; American Type Culture Collection) and the malignant glioma cell line U343MGaCl2:6 (*28*) (denoted U343) were used in all cell experiments. This A431 cell line is reported to express approximately 2×10^6 EGFRs per cell, and the U343 cell line expresses approximately 5.5×10^5 EGFRs per cell. The cells were cultured in Ham's F10 medium (Biochrom Kg), supplemented with 10% fetal calf serum (Sigma), L-glutamine (2 mmol/L), and PEST (penicillin 100 IU/mL and streptomycin 100 μg/mL), both from Biochrom Kg. During cell culture and cell experiments (unless otherwise stated), cells were grown at 37°C in incubators with humidified air, equilibrated with 5% CO_2. The cells were trypsinized with trypsin–ethylenediaminetetraacetic acid (EDTA) (0.25% trypsin, 0.02% EDTA in PBS without Ca and Mg) from Biochrom Kg.

Binding of ^{68}Ga-DOTA-hEGF to Cells

A431 and U343 cells were cultured in 3-cm Petri dishes (approximately 3.5×10^5 and 1.9×10^5 cells per dish, respectively). Triplicate cell dishes were used for each measuring point. After washing the cells once, 1 mL of ^{68}Ga-DOTA-hEGF in cell culture medium (35 ng/dish, 50 kBq/dish for A431 cells and 5 ng/dish, 20 kBq/dish for U343 cells) was added. To some dishes, a molar excess of hEGF (5 or 3 μg/dish) was added together with the labeled conjugate to estimate the binding specificity of the ^{68}Ga-DOTA-hEGF conjugate. After 0.5- to 6-h incubation at 37°C, the cells were washed 6 times with cold serum-free medium, and they were then harvested using 0.5 mL of trypsin-EDTA (15 min, 37°C). The trypsination was terminated with addition of 1 mL of cell culture medium, and part of the cell suspension (0.5 mL) was used for cell counting, whereas the rest was measured in a γ-counter.

To estimate the cellular internalization of the ^{68}Ga-DOTA-hEGF conjugate, several additional cell dishes were used during the binding study to separate the membrane-bound fraction of the conjugate from internalized radioactivity. Instead of trypsinizing the cells, treatment with 0.5 mL of ice-cold 0.1 mol/L glycine-HCl buffer, pH 2.5, for 6 min at 0°C was used to extract the membrane-bound fraction of the conjugate. An additional 0.5 mL of the glycine-HCl buffer was used to wash the cells once. The remaining radioactivity, considered to be internalized radioactivity, was collected by treatment with 0.5 mL of 1 mol/L NaOH solution at 37°C for about 60 min. Another 0.5 mL of NaOH solution was used for washing. The collected fractions were measured in an automated γ-counter.

The binding of ^{68}Ga-DOTA-hEGF to A431 cells and U343 cells on ice was also studied to determine the time required for binding in the saturation study. Cell dishes placed on ice were incubated with ice-cold ^{68}Ga-DOTA-hEGF solution for 0.5–4 h. The cells were then washed, trypsinized, and counted as described.

Cellular Retention of Radioactivity

The cellular retention of radioactivity was studied after 1 h of incubation with ^{68}Ga-DOTA-hEGF. After the incubation was interrupted, the cells were washed thoroughly to eliminate unbound conjugate, and the incubation was then continued in fresh cell culture medium. After 0.5–4 h, the cells were trypsinized, counted, and measured for radioactivity, as described.

Saturation Assay and Estimation of Dissociation Constant, K_d

The equilibrium K_d was determined from a saturation study with ^{68}Ga-DOTA-hEGF on A431 cells and U343 cells. Cells cultured in 24-well plates (approximately 3.1×10^4 A431 cells/well and 7.8×10^4 U343 cells/well) were placed on ice, and ice-cold ^{68}Ga-DOTA-hEGF solutions of different concentrations (0.26–16.9 nmol/L for A431 and 0.14–36 nmol/L for U343, 0.5 mL/well) were added. For each concentration, the nonspecific background binding was studied by adding a 100 times excess of unlabeled hEGF to some wells. After 2 h of incubation (the time was determined from the results of the uptake study on ice), the cells were washed 6 times with cold serum-free medium. The cells were then trypsinized with 0.5 mL of trypsin-EDTA (15 min at 37°C), and the cells were counted and measured for radioactivity in a γ-counter.

Animal Tumor Model

The in vivo studies were performed in adult female BALB/c *nu/nu* mice (21–25 g) (Möllegård) with tumor xenografts. All animals were handled according to the guidelines by the Swedish Animal Welfare Agency, and the experiments were approved by the local Ethics Committee for Animal Research. The mice were injected subcutaneously with A431 tumor cells (approximately 7 million cells per tumor in 100 μL of cell culture medium) in both front legs. The tumors were allowed to grow for 12–13 d before the experiments were performed and had then reached a weight of 0.1–0.8 g.

Biodistribution in Mice with A431 Tumor Xenografts

Mice with A431 tumor xenografts were injected intravenously with 50 μL of ^{68}Ga-DOTA-hEGF solution (0.16 nmol or 0.016 nmol in PBS per animal; 4 animals in each group), and 30 min after injection the animals were sacrificed and dissected. The mice were anesthetized by an intraperitoneal injection of a mixture of Rompun (Bayer Co.; 1 mg/mL) and Ketalar (Parke Davis; 10 mg/mL), 0.2 mL/10 g of animal weight, and killed by heart puncture. In addition to the tumors, the blood, heart, pancreas, spleen, stomach, liver, kidneys, lungs, small and large intestine, muscle, bone, and salivary gland were collected, weighed, and measured in an automated γ-counter. The tails were also measured for radioactive content to determine the accuracy of the injections. Organ values were calculated as the percentage of injected dose per gram of organ (%ID/g).

microPET

Imaging was performed on a microPET R4 scanner (Concorde Microsystems, Inc.). Mice with A431 tumor zenografts were anesthetized with isoflurane (Baxter Medical AB) inhalation. ^{68}Ga-DOTA-hEGF was injected via a tail vein (2.0 ± 0.5 MBq in 100 μL followed by 50 μL of saline). The mice were imaged (1 bed position; filtered-backprojection reconstruction; image resolution of 2 mm) for 30 or 120 min. microPET images were corrected for decay and attenuation. Regions of interest (ROIs) were drawn on

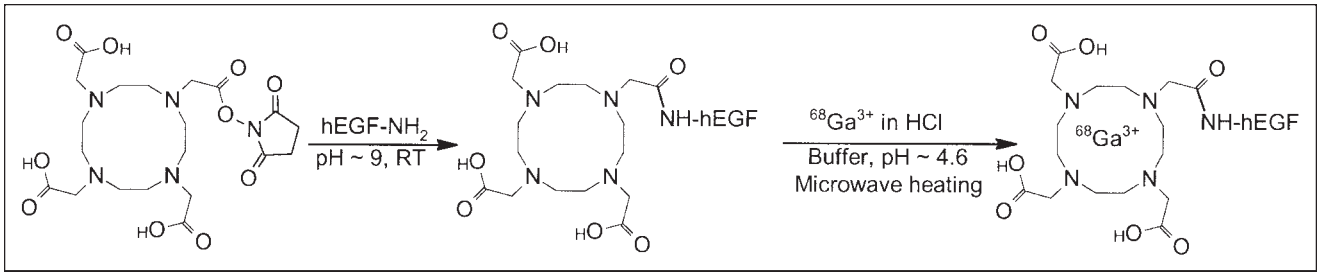

FIGURE 1. Reaction scheme for conjugation of DOTA to hEGF using a commercial *N*-hydroxysulfosuccinimide ester of DOTA and subsequent microwave-accelerated complexation of ^{68}Ga with DOTA-hEGF. RT = room temperature.

liver, kidney, bladder, salivary gland, and tumor using ASIpro software (Concorde Microsystems, Inc.). Pharmacokinetic curves, representing the radioactivity concentrations (Bq/cm^3 of tissue) versus time after injection, were acquired by drawing ROIs in the selected organs. The uptake index was calculated as radioactivity in organ (kBq/mL)/injected activity (kBq) × 100%.

RESULTS

Chemistry and Radiochemistry of ^{68}Ga-DOTA-hEGF Preparation

^{68}Ga-DOTA-hEGF was synthesized by a 2-step procedure, where hEGF was initially conjugated to a bifunctional chelator, DOTA, and thereafter labeled with ^{68}Ga via a complexation reaction of ^{68}Ga with the chelator (*24,27*). In the conjugation step, one of the carboxylic groups of the DOTA chelate was coupled to an amine functionality of the peptide, forming an amide bond (Fig. 1). hEGF contains 1 terminal and 2 lysine amino groups. Consequently, the conjugation reaction of hEGF resulted in the formation of a mixture of molecules with 1, 2, and 3 DOTA fragments, as determined by LC-ESI-MS analysis.

The microwave-accelerated labeling of the conjugates (Fig. 1) was performed by use of a nonconcentrated or a preconcentrated generator ^{68}Ga-eluate (*24*) with respective radioactivity incorporation of 60% ± 10% (n = 3) and 77% ± 4% (n = 3). The attachment of ^{68}Ga to hEGF was DOTA mediated, as the same treatment of nonconjugated hEGF did not provide any labeled peptide. The radiochemical purity of the tracers in the study exceeded 95%. The tracer proved to be stable in the PBS during the stability assay of 4 h with no additional radio-HPLC signals.

Cell-Binding and Retention Experiments

The binding specificity of ^{68}Ga-DOTA-EGF to EGFR-expressing cervical carcinoma A431 and glioma U343 cell lines in vitro is shown in Figure 2. To demonstrate that the binding was receptor specific, a large amount of unlabeled hEGF was added to cells in the control experiments to saturate the EGFR. Results of the binding specificity experiments demonstrated that the binding of ^{68}Ga-DOTA-hEGF to both cell lines could be prevented by receptor saturation at all tested data points.

The results of the saturation experiments with ^{68}Ga-DOTA-hEGF on cervical carcinoma A431 and glioma U343 cells are shown in Figures 3A and 3B, respectively. The specific binding (amol/cell) was plotted against the total molar concentration of added radiolabeled conjugate, and the result was analyzed by nonlinear regression using the GraphPad Prism Software. Both curves seem to have reached a maximum value, indicating saturation. The obtained K_d values were in an excellent agreement, 2.0 nmol/L for A431 cells and 2.3 nmol/L for U343 cells. The number of binding sites per cell could be calculated from the B_{max} value. The obtained number, 7.8×10^5 sites per U343 cell, corresponds reasonably well with 5.4×10^5 as previously determined for a ^{111}In-Bz-DTPA-hEGF conjugate (DTPA is diethylenetriaminepentaacetic acid) (*20*). The number of binding sites for A431, 1.9×10^6 EGFR per cell, was also in good agreement with literature data.

The degree of internalization was estimated by acid wash. Radioactivity that was removed from cells by an acidic buffer was considered membrane bound and the rest was

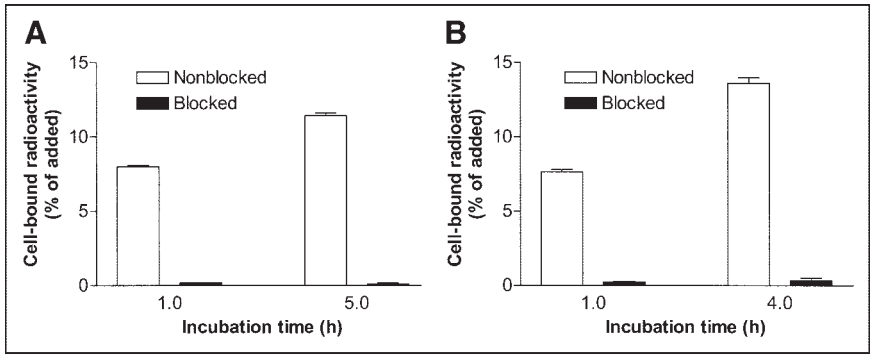

FIGURE 2. Specificity of ^{68}Ga-DOTA-hEGF binding to A431 carcinoma (A) and U343 glioma (B) cell lines. At all time points, EGFR binding was blocked with excess of unlabeled hEGF. Binding was specific, as it could be suppressed. Data are presented as mean ± SD (n = 3).

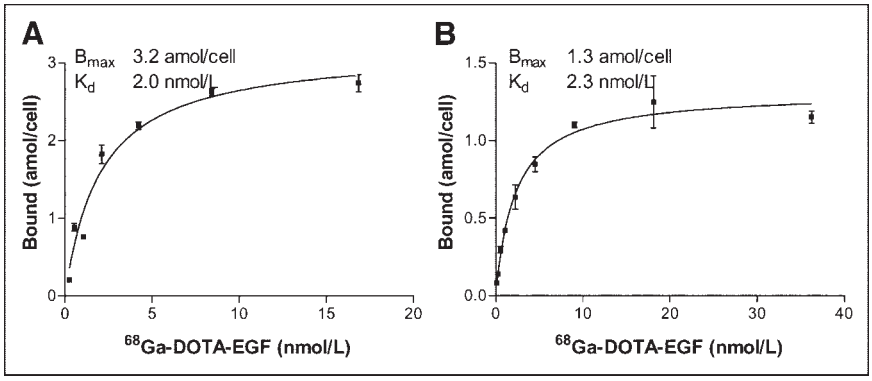

FIGURE 3. Saturation of ^{68}Ga-DOTA-hEGF binding to cultured carcinoma A431 (A) and glioma U343 (B) cells. Cells were incubated with different concentrations of ^{68}Ga-DOTA-hEGF (0.26–16.9 nmol/L for A431 cells and 0.14–36 nmol/L for U343 cells) for 2 h on ice. Data are presented as mean ± SD (n = 3).

considered internalized. The results summarized in Figure 4 show that internalization of ^{68}Ga-DOTA-hEGF was a rapid process in both cell lines. However, the internalization rate was faster in glioma U343 cells than in A431 cells. More than 50% of the radioactivity was internalized 30 min after the start of incubation in glioma U343 cells.

The retention pattern of radioactivity after interrupted incubation with ^{68}Ga-DOTA-hEGF for A431 and U343 cells was similar for both cell lines (Fig. 5). An initial drop of radioactivity, which was most probably due to dissociation of membrane-bound conjugates, was followed by a relatively constant amount of cell-bound ^{68}Ga. Both cell lines demonstrated good retention, with >70% of the radioactivity still cell associated 4 h (3 half-lives of the label) after interrupted incubation.

Biodistribution Studies

A summary of the biodistribution data for ^{68}Ga-DOTA-hEGF in A431 tumor-bearing mice is shown in Figure 6. The measurement of the organ radioactivity 30 min after intravenous administration of ^{68}Ga-DOTA-hEGF showed the highest values in the kidneys and liver, followed by pancreas, salivary gland, small and large intestine, stomach, and spleen. The uptake of ^{68}Ga-DOTA-hEGF in the A431 tumor xenograft was 1.51 ± 0.16 %ID/g and 2.69 ± 0.29 %ID/g, for 0.016 and 0.16 nmol of injected conjugate, respectively (P = 0.036). The radiotracer had a rapid blood clearance, with <1 %ID/g remaining in the circulation at the 30-min time point. There was a statistically significant decrease in the radioactivity uptake in pancreas, spleen, and stomach when 0.16 nmol of conjugate was injected. There was a statistically significant increase of tumor-to-organ ratios for heart, pancreas, stomach, spleen, lungs, intestines, muscles, and salivary glands when 0.16 nmol of conjugate was injected. However, there was no difference in tumor-to-blood ratio, 4.42 ± 1.81 %ID/g and 4.50 ± 2.53 %ID/g, for 0.016 and 0.16 nmol of injected conjugate, respectively (P = 0.036).

microPET

The localization of ^{68}Ga-DOTA-hEGF in tumor-bearing mice as determined by microPET imaging (Fig. 7) was

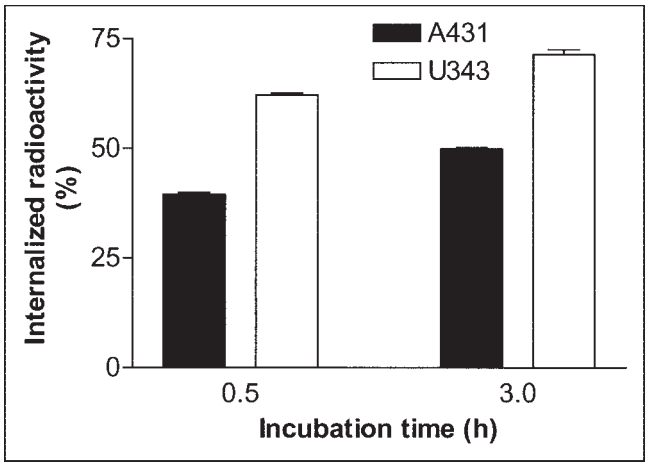

FIGURE 4. Internalization of ^{68}Ga-DOTA-hEGF after binding to carcinoma A431 and glioma U343 cells. Internalization was determined by acid wash. y-Axis presents percentage of the total cell-associated radioactivity. Data are presented as mean ± SD (n = 3).

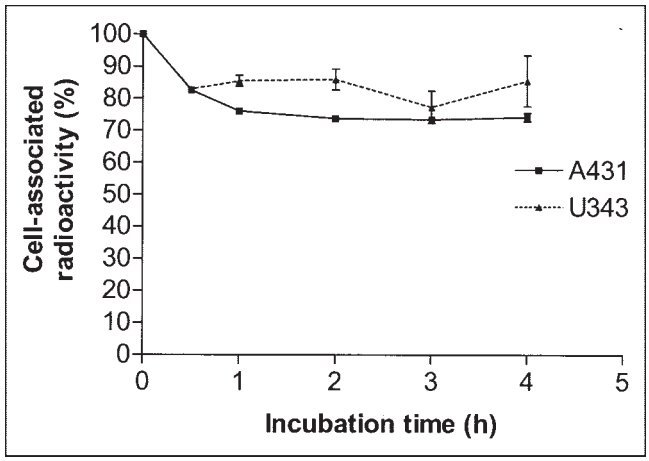

FIGURE 5. Cell-associated ^{68}Ga radioactivity as function of time after interrupted incubation of A431 (solid line) and U343 (dotted line) cells with ^{68}Ga-DOTA-hEGF. Cell-associated radioactivity at time zero after interrupted incubation was considered as 100%. Data are presented as mean ± SD (n = 3). Both A431 and U343 cell cultures were incubated with ^{68}Ga-DOTA-hEGF for 4 h.

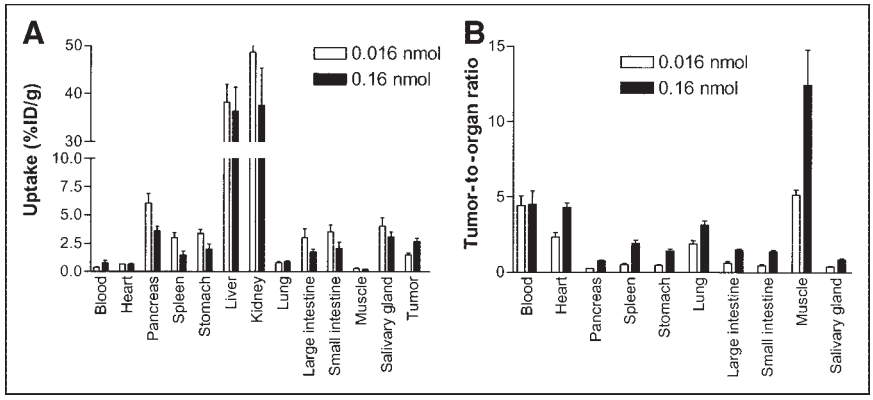

FIGURE 6. (A) Biodistribution of ^{68}Ga-DOTA-hEGF expressed as %ID/g tissue in tumor-bearing nude mice at 30-min time point. (B) Tumor-to-organ ratios of ^{68}Ga-DOTA-EGF in tumor-bearing nude mice at 30-min time point. Mice were intravenously injected with either 0.016 or 0.16 nmol of radiotracer and killed at 30-min time point. Data are presented as mean ± SD (n = 4).

followed by radioactivity measurements of blood, liver, kidney, and both tumor samples collected after decapitation of the animal.

The image of a tumor-bearing mouse 30 min after administration of 2.0 MBq ^{68}Ga-DOTA-hEGF with a specific radioactivity (SRA) of 12–20 MBq/nmol is shown in Figure 7A. The results of the microPET image were correlated with the radioactivity measurements of blood, liver, and kidney samples. Both right and left leg tumors were visible with clear contrast against the adjacent background. Prominent uptake was observed in the liver and kidneys, and clearance of the radioactivity through the urinary bladder was evident (Fig. 8). The distribution to tumors and salivary gland was slower. Uptake data derived from microPET and biodistribution studies were found to be in agreement with data obtained from the tissue sampling after imaging.

DISCUSSION

The experience with somatostatin analogs shows that the use of macrocyclic chelators, such as DOTA derivatives, may provide an adequate in vivo stability of the ^{68}Ga radiolabel (*25*). On the other hand, macrocyclic chelators are kinetically inert, and incorporation of radiometals into DOTA requires elevated temperatures (approximately 100°C) or a long chelating procedure. Both of these approaches are undesirable because of the potential damage to the targeting peptide and the relatively short half-life of ^{68}Ga. Microwave heating is an attractive tool that provides acceleration of the labeling. This technique has been used for labeling different organic molecules with ^{131}I, ^{11}C, ^{15}O, ^{18}F, and ^{13}N (*29*). Earlier, we have demonstrated the potential of microwave heating for speeding up ^{68}Ga complexation with DOTA bifunctional chelator coupled to oligonucleotides and peptides (*24,26,27*). For this reason, the use of the microwave technique was applied in this study. The method made it possible to perform labeling within 1 min with both nonconcentrated and preconcentrated generator eluate. ^{68}Ga incorporation was satisfactory (60% ± 10%) when using the peak fraction of the nonconcentrated generator eluate. However, about 40% of the ^{68}Ga activity was wasted. The preconcentration of the generator eluate provided use of 85%–90% of the initially available radioactivity and increased radioactivity incorporation (approximately 80%). Consequently, the SRA of the tracer was increased as well. Previously, ^{68}Ga labeling under microwave heating was performed with small peptides with a molecular weight varying between 1.4 and 3.7 kDa (*24,27*). The binding

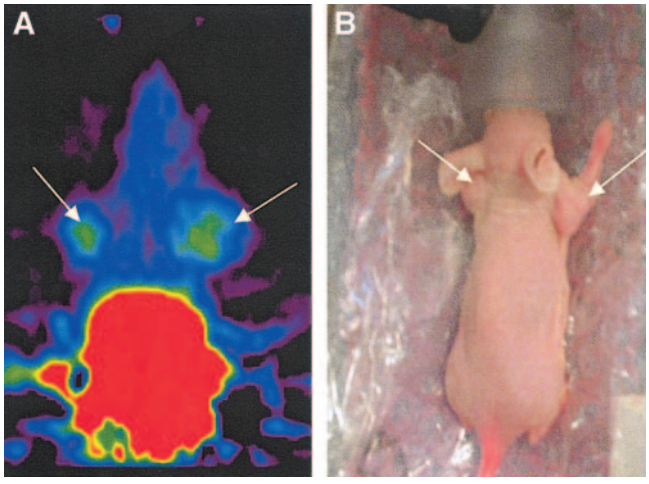

FIGURE 7. (A) Image shows summation of frames 20–24 (20–30 min after injection). Tumors (arrows) can clearly be seen at either side of head. (B) Photograph of positioning of mouse.

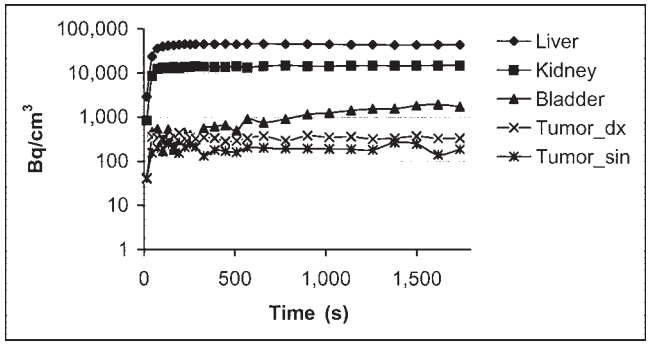

FIGURE 8. Pharmacokinetic curves show rapid distribution of ^{68}Ga-DOTA-hEGF (0.16 nmol injected) to liver, kidney, bladder, and tumors. Tumor_dx = right side tumor; Tumor_sin = left side tumor.

properties of hEGF are determined by a more complex structure and, therefore, could be more vulnerable to the action of microwave heating. Thus, a careful characterization of the labeled conjugate was required. Initial experiments demonstrated that after microwave-assisted labeling, ^{68}Ga-DOTA-hEGF retained its capacity to bind to the EGFR-expressing cell lines A431 and U343. This binding was receptor specific, as it could be precluded by presaturation of EGFR with an unlabeled ligand (Fig. 2). Affinity measurements showed a K_d of about 2 nmol/L for both cell lines (Fig. 3). This value was in good agreement with values obtained for hEGF-chelator conjugates labeled with indium or lutetium without microwave heating (*20,30*). This demonstrated that the use of microwaves did not deteriorate the receptor-binding properties of such a complex peptide as hEGF. The affinity in the low nanomolar range was also compatible with the application of ^{68}Ga-DOTA-hEGF as a tracer for in vivo imaging.

The internalization of the targeting conjugate is considered as an important property because it prevents its eventual dissociation from cancer cells in vivo. The use of the hEGF–EGFR system for targeting should meet this requirement, as internalization of the receptor–ligand complex is well documented for this system. Indeed, the internalization study demonstrated that ^{68}Ga-DOTA-hEGF was internalized by both model cell lines (Fig. 4). Internalization by U343 cells seems to be more rapid than internalization by A431 cells, which might be explained by the difference in cellular processing machinery of these 2 cell lines.

Good intracellular retention of radiometals after internalization was considered when we designed the EGFR-targeting conjugate. The retention studies (Fig. 5) confirmed good retention of ^{68}Ga-DOTA-hEGF by both cell lines. The high cellular retention of ^{68}Ga-DOTA-hEGF was also in good agreement with data relating to ^{111}In- and ^{177}Lu-labeled hEGF-chelator conjugates (*15,20,30*).

Although the in vitro properties of ^{68}Ga-DOTA-hEGF were promising, an ultimate proof of the concept may be provided only by in vivo experiments such as microPET imaging and biodistribution. The feasibility of EGFR-expressing tumor imaging using ^{68}Ga-DOTA-hEGF was demonstrated by microPET (Fig. 7). The tracer localization was rapid, and the plateau of accumulation in tumors, liver, and kidneys was reached within 10 min after injection. Besides tumors, high radioactivity uptake was observed in kidneys and liver. A high kidney uptake is typical for all radioconjugates, which are small enough to pass through glomerular membranes and hydrophilic enough to undergo renal clearance (*31*). A predominant renal clearance was also confirmed in this study by the high level of radioactivity accumulation in the urinary bladder. Radioactivity accumulation in the urinary bladder peaked at about 30 min after injection, indicating that, at this moment, the blood elimination phase was essentially accomplished. Another organ with high radioactivity uptake was the liver. It has been demonstrated earlier in several studies that liver uptake is EGFR mediated (*30,32*). High liver uptake is one of the limitations of ^{68}Ga-DOTA-hEGF because it might prevent imaging of EGFR expression in hepatic metastases. However, we believe that ^{68}Ga-DOTA-hEGF might be helpful for imaging of EGFR expression in primary tumors of NSCLC. The lesion is in this case placed at some distance from liver, and EGFR expression in NSCLC has been imaged earlier using ^{131}I-hEGF. Expression of EGFR is a precondition for EGFR-targeting therapy using, for example, cetuximab (*33*). Moreover, heterogenicity of EGFR expression in NSCLC makes biopsy a less-reliable procedure (*33*). The use of ^{68}Ga-DOTA-hEGF in combination with PET/CT might help to determine the eligibility of a given patient for cetuximab therapy by evaluation of EGFR overexpression in the whole tumor. The biodistribution studies revealed the influence of SRA on radioactivity uptake in tumors and normal organs. The injection of ^{68}Ga-DOTA-hEGF with lower SRA resulted in the tumor uptake of 2.7 ± 0.3 %ID/g, which is comparable with the accumulation in murine xenografts of such a well-established radiopharmaceutical as ^{111}In-OctreoScan (about 3 %ID/g) (*34*). However, it remains to be investigated if it is possible to block the liver uptake (*32*) by manipulating the SRA of ^{68}Ga-DOTA-hEGF. High SRA, achieved by using a combination of the preconcentration of ^{68}Ga and microwave heating, enables such investigation of the gaussian distribution of radioactivity uptake as a function of SRA (*35,36*). Furthermore, the optimization of SRA might be performed for future patient studies.

CONCLUSION

hEGF conjugated with a macrocyclic DOTA-chelating group and radiolabeled with the positron-emitting radionuclide ^{68}Ga showed high EGFR-binding affinity and specificity and a rapid internalization in both carcinoma A431 and glioma U343 cells. The localization of ^{68}Ga-DOTA-hEGF in A431 tumor xenografts and EGFR-positive tissues was shown in both biodistribution and microPET imaging studies. ^{68}Ga-DOTA-hEGF as a peptide-based tracer met the major requirements, such as tissue permeability, high-affinity receptor binding, and a rapid clearance from the body. Further investigations are required to determine the optimal SRA for imaging. ^{68}Ga-DOTA-hEGF might be useful for the selection of patients for EGFR-targeting therapy as well as evaluation of response to such therapy.

ACKNOWLEDGMENTS

The Swedish Research Council is acknowledged for its support (grant K3464). Financial support was partially given by the Swedish Cancer Society. The authors thank the staff of the Unit of Biomedical Radiation Sciences, Uppsala University, for helpful assistance in the biodistribution studies.

REFERENCES

1. Yarden Y, Sliwkowski MX. Untangling the ErbB signalling network. *Nat Rev Mol Cell Biol.* 2001;2:127–137.

2. Collins VP. Amplified genes in human gliomas. *Semin Cancer Biol.* 1993;4:27–32.
3. Bigner SH, Burger PC, Wong AJ, et al. Gene amplification in malignant human gliomas: clinical and histopathologic aspects. *J Neuropathol Exp Neurol.* 1988; 47:191–205.
4. Walker RA, Dearing SJ. Expression of epidermal growth factor receptor mRNA and protein in primary breast carcinomas. *Breast Cancer Res Treat.* 1999;53: 167–176.
5. Witton CJ, Reeves JR, Going JJ, Cooke TG, Bartlett JM. Expression of the HER1–4 family of receptor tyrosine kinases in breast cancer. *J Pathol.* 2003; 200:290–297.
6. Hirsch FR, Varella-Garcia M, Bunn PA Jr, et al. Epidermal growth factor receptor in non-small-cell lung carcinomas: correlation between gene copy number and protein expression and impact on prognosis. *J Clin Oncol.* 2003;21: 3798–3807.
7. Castillo L, Etienne-Grimaldi MC, Fischel JL, Formento P, Magne N, Milano G. Pharmacological background of EGFR targeting. *Ann Oncol.* 2004;15:1007–1012.
8. Tsutsui S, Kataoka A, Ohno S, Murakami S, Kinoshita J, Hachitanda Y. Prognostic and predictive value of epidermal growth factor receptor in recurrent breast cancer. *Clin Cancer Res.* 2002;8:3454–3460.
9. Selvaggi G, Novello S, Torri V, et al. Epidermal growth factor receptor overexpression correlates with a poor prognosis in completely resected non-small-cell lung cancer. *Ann Oncol.* 2004;15:28–32.
10. Dadparvar S, Krishna L, Miyamoto C, et al. Indium-111-labeled anti-EGFr-425 scintigraphy in the detection of malignant gliomas. *Cancer.* 1994;73:884–889.
11. Vallis KA, Reilly RM, Chen P, et al. A phase I study of ^{99m}Tc-hR3 (DiaCIM), a humanized immunoconjugate directed towards the epidermal growth factor receptor. *Nucl Med Commun.* 2002;23:1155–1164.
12. Schechter NR, Wendt RE, Yang DJ, et al. Radiation dosimetry of ^{99m}Tc-labeled C225 in patients with squamous cell carcinoma of the head and neck. *J Nucl Med.* 2004;45:1683–1687.
13. Blomquist E, Carlsson J. Strategy for planned radiotherapy of malignant gliomas: postoperative treatment with combinations of high-dose proton irradiation and tumor seeking radionuclides. *Int J Radiat Oncol.* 1992;22:259–263.
14. Cuartero-Plaza A, Martinez-Miralles E, Rosell R, Vadell-Nadal C, Farre M, Real FX. Radiolocalization of squamous lung carcinoma with ^{131}I-labeled epidermal growth factor. *Clin Cancer Res.* 1996;2:13–20.
15. Orlova A, Bruskin A, Sjostrom A, Lundqvist H, Gedda L, Tolmachev V. Cellular processing of ^{125}I- and ^{111}In-labeled epidermal growth factor (EGF) bound to cultured A431 tumor cells. *Nucl Med Biol.* 2000;27:827–835.
16. Reilly RM, Gariepy J. Factors influencing the sensitivity of tumor imaging with a receptor-binding radiopharmaceutical. *J Nucl Med.* 1998;39:1036–1043.
17. Capala J, Barth RF, Bailey MQ, Fenstermaker RA, Marek MJ, Rhodes BA. Radiolabeling of epidermal growth factor with ^{99m}Tc and in vivo localization following intracerebral injection into normal and glioma-bearing rats. *Bioconjug Chem.* 1997;8:289–295.
18. Babaei MH, Almqvist Y, Orlova A, Shafii M, Kairemo K, Tolmachev V. [^{99m}Tc]HYNIC-hEGF, a potential agent for imaging of EGF receptors in vivo: preparation and pre-clinical evaluation. *Oncol Rep.* 2005;13:1169–1175.
19. Hnatowich DJ, Qu T, Chang F, Ley AC, Ladner RC, Rusckowski M. Labeling peptides with technetium-99m using a bifunctional chelator of a N-hydroxysuccinimide ester of mercaptoacetyltriglycine. *J Nucl Med.* 1998;39:56–64.
20. Sundberg AL, Orlova A, Bruskin A, et al. [^{111}In]Bz-DTPA-hEGF: preparation and in vitro characterization of a potential anti-glioblastoma targeting agent. *Cancer Biother Radiopharm.* 2003;18:643–654.
21. Lundqvist H, Lubberink M, Tolmachev V. Positron emission tomography. *Eur J Phys.* 1999;19:537–552.
22. Lundqvist H, Tolmachev V. Targeting peptides and positron emission tomography. *Biopolymers.* 2002;66:381–392.
23. Maecke HR, Hofmann M, Haberkorn U. ^{68}Ga-Labeled peptides in tumor imaging. *J Nucl Med.* 2005;46(suppl 1):172S–178S.
24. Velikyan I, Beyer GJ, Langstrom B. Microwave-supported preparation of ^{68}Ga bioconjugates with high specific radioactivity. *Bioconjug Chem.* 2004;15:554–560.
25. Maecke HR. Radiolabeled peptides in nuclear oncology: influence of peptide structure and labeling strategy on pharmacology. Ernst Schering Research Foundation Workshop. 2005:43–72.
26. Velikyan I, Lendvai G, Valila M, et al. Microwave accelerated Ga-68-labelling of oligonucleotides. *J Labelled Compds Radiopharm.* 2004;47:79–89.
27. Lavén M, Velikyan I, Djodjic M, et al. Imaging of peptide adsorption to microfluidic channels in a plastic compact disc using a positron emitting radionuclide. *Lab on a Chip.* 2005;5:756–763.
28. Westermark B, Magnusson A, Heldin CH. Effect of epidermal growth factor on membrane motility and cell locomotion in cultures of human clonal glioma cells. *J Neurosci Res.* 1982;8:491–507.
29. Elander N, Jones JR, Lu SY, Stone-Elander S. Microwave-enhanced radiochemistry. *Chem Soc Rev.* 2000;29:239–249.
30. Sundberg AL, Gedda L, Orlova A, et al. [^{177}Lu]Bz-DTPA-EGF: preclinical characterization of a potential radionuclide targeting agent against glioma. *Cancer Biother Radiopharm.* 2004;19:195–204.
31. Behr TM, Goldenberg DM, Becker W. Reducing the renal uptake of radiolabeled antibody fragments and peptides for diagnosis and therapy: present status, future prospects and limitations. *Eur J Nucl Med.* 1998;25:201–212.
32. Tolmachev V, Orlova A, Wei Q, Bruskin A, Carlsson J, Gedda L. Comparative biodistribution of potential anti-glioblastoma conjugates [^{111}In]DTPA-hEGF and [^{111}In]Bz-DTPA-hEGF in normal mice. *Cancer Biother Radiopharm.* 2004;19: 491–501.
33. Dubey S, Schiller JH. Three emerging new drugs for NSCLC: pemetrexed, bortezomib, and cetuximab. *Oncologist.* 2005;10:282–291.
34. Froidevaux S, Heppeler A, Eberle AN, et al. Preclinical comparison in AR4-2J tumor-bearing mice of four radiolabeled 1,4,7,10-tetraazacyclododecane-1,4,7,10-tetraacetic acid-somatostatin analogs for tumor diagnosis and internal radiotherapy. *Endocrinology.* 2000;141:3304–3312.
35. de Jong M, Breeman WA, Bernard BF, et al. Tumour uptake of the radiolabelled somatostatin analogue [DOTA^0,TYR^3]octreotide is dependent on the peptide amount. *Eur J Nucl Med.* 1999;26:693–698.
36. Bernhardt P, Kolby L, Johanson V, Nilsson O, Ahlman H, Forssell-Aronsson E. Biodistribution of ^{111}In-DTPA-D-Phe1-octreotide in tumor-bearing nude mice: influence of amount injected and route of administration. *Nucl Med Biol.* 2003; 30:253–260.